Supplement of Geosci. Model Dev. Discuss., 7, 6549–6626, 2014
http://www.geosci-model-dev-discuss.net/7/6549/2014/
doi:10.5194/gmdd-7-6549-2014-supplement

Geoscientific Model Development Discussions
Open Access

Supplement of

Quantitative evaluation of ozone and selected climate parameters in a set of EMAC simulations

M. Righi et al.

Correspondence to: M. Righi (mattia.righi@dlr.de)

In this supplement, we provide additional information on the EMAC model simulations (Section S1) as well as additional figures to support the discussion in the paper (Section S2).

S1 Additional information on EMAC simulations

All four model setups consider boundary conditions for long-lived species, supplied to the model via the TNUDGE submodel (Kerkweg et al., 2006) and including greenhouse gases CO_2, N_2O, CH_4, chlorofluorocarbons ($CFCl_3$, CF_2Cl_2, CH_33CCl_3, CCl_4), hydrochlorofluorocarbons (CH_3Cl, CH_3Br), halons (CF_2ClBr, CF_3Br) and H_2. The input fields (monthly-mean, zonally averaged mixing ratios) are taken from the AGAGE database (Prinn et al., 2000). Emissions of short-lived species (NO, CO, SO_2, NH_3 and NMHCs C_2H_4, C_2H_6, C_3H_6, C_3H_8, C_4H_{10}, CH_3CHO, CH_3COCH_3, CH_3COOH, CH_3OH, HCHO, HCOOH), methyl ethyl ketone (MEK)) are provided to the model as offline fields via the OFFLEM/OFFEMIS submodel (Kerkweg et al., 2006). We consider anthropogenic (traffic and non-traffic) source from different datasets, and natural sources like volcanic SO_2 (from AeroCom; Dentener et al., 2006), terrestrial DMS (Spiro et al., 1992) and biogenic sources (Guenther et al., 1995).

NMHC speciation is realized according to the speciation fraction by von Kuhlmann et al. (2003). Different fractions are used for biomass burning and anthropogenic emissions. NMHC mass (usually kg(NMHC)) is converted to carbon mass (kg(C)) assuming a ratio of 161/210, as suggested in the IPCC third assessment report (see also Hoor et al., 2009). In a test simulation (not discussed here), the speciation provided in the inventory by Lamarque et al. (2010) has also been considered, but due to its inconsistency with the chemical mechanism of our model, it led to unrealistic results in comparison with the tropospheric vertical profiles from Emmons et al. (2000). Therefore the above method was preferred and applied in all of the simulations presented here. Anthropogenic (except aviation) and biomass burning emissions are distributed in the vertical using 6 layers (45, 140, 240, 400, 600, 800 m) following the suggestions of Pozzer et al. (2009), mostly based on EMEP. Aviation emission levels are provided by the corresponding inventory (in the range 0-15 km). Volcanic emissions are distributed according to the volcano height. Other sources are emitted as two-dimensional surface fluxes and no assumption on the injection height is therefore required.

The model also simulates online emissions of isoprene and soil NO, via the ONLEM/ONEMIS submodel. The exchange of species between the atmosphere and the ocean is simulated by the AIRSEA submodel (Pozzer et al., 2006), based on the concentration of isoprene (Broadgate et al., 1997), oceanic DMS (Kettle and Andreae, 2000) as well as the ocean salinity (Boyer et al., 2002). Solar cycle data for the calculation of the photolysis rates in the JVAL submodel are taken from Lean (2000). Finally, lightning NO_x emissions are calculated online by the LNOX submodel using different parametrization. A summary of boundary conditions, emissions and other data required by the model in the four setups is given in Table S1. The simulations discussed here do not include aerosols, therefore the standard ECHAM5 aerosol climatology (Tanre et al., 1994) is used to drive the radiation calculations.

Table S1: Boundary conditions and emission datasets for the EMAC simulations. References to each dataset/inventory are given in the text. A specification whether data are used in transient or in constant (2000) mode is given for each dataset. The abbreviation SB97 refers to the inventory by Schmitt and Brunner (1997). M7 is the aerosol model by Vignati et al. (2004) providing aerosol surface concentrations for heterogeneous chemistry reactions.

	MESSy submodel	EVAL2	QCTM	TS2000	ACCMIP
Concentrations of long-lived species	TNUDGE	AGAGE			
		Transient	Transient	2000	2000
Biomass burning	OFFLEM/	GFED	GFED	CMIP5	CMIP5
emissions	OFFEMIS	Transient	Transient	2000	2000
Agric. waste burning	OFFLEM/	CMIP5			
emissions	OFFEMIS	2000	2000	2000	2000
Anthrop. non-traffi	OFFLEM/	CMIP5			
emissions	OFFEMIS	2000	2000	2000	2000
Land transport	OFFLEM/	QUANTIFY	QUANTIFY	CMIP5	CMIP5
emissions	OFFEMIS	2000	2000	2000	2000
Shipping	OFFLEM/	CMIP5			
emissions	OFFEMIS	Transient	Transient	2000	2000
Aviation	OFFLEM/	SB97	QUANTIFY	QUANTIFY	CMIP5
emissions	OFFEMIS	Transient	2000	2000	2000
Biogenic	OFFLEM/	Guenther et al. (1995)			
emissions	OFFEMIS	2000	2000	2000	2000
Volcanic	OFFLEM/	AeroCom			
emissions	OFFEMIS	2000	2000	2000	2000
Terrestrial DMS	OFFLEM/	Spiro et al. (1992)			
emissions	OFFEMIS	2000	2000	2000	2000
NH_3	OFFLEM/	EDGAR	EDGAR	CMIP5	CMIP5
emissions	OFFEMIS	2000	2000	2000	2000
Isoprene emissions	AIRSEA	Broadgate et al. (1997)			
Oceanic DMS emissions	AIRSEA	Kettle and Andreae (2000)			
Ocean salinity	AIRSEA	Boyer et al. (2002)			
Aerosol (radiation)	–	Tanre et al. (1994)			
Aerosol (chemistry)	–	M7	Not included		
QBO	QBO	Giorgetta and Bengtsson (1999)		Not included	
Solar cycle	JVAL	Lean (2000)			
		Transient	2000	2000	2000
Lightning NO_x	LNOX	Price and Rind (1994)		Grewe et al. (2001)	
Nudging	–	ECMWF		Not included	

Table S2: Total emissions for different species and sectors in the four EMAC simulations. For transient emissions, minimum and maximum values for the simulated period (excluding the spin-up year) are given. For constant emission, the value refers to the year 2000, whereas for online emissions the average value is provided. Natural sources emissions of NO_x include also lightning emissions, given in brackets in the corresponding column. Units are Tg(species)/yr and Tg(NO)/yr for NO_x. See Table S1 for the corresponding emission inventories. NH_3 emissions per sector are available only for the ACCMIP run, in the other cases only the total value is given in the last row.

Sector	**Experiment**	**NO_x**	**CO**	**SO_2**	**NH_3**	**C_2H_4**	**C_2H_6**	**C_3H_6**	**C_3H_8**
Biomass and agric. waste burning	EVAL2	7.87 – 11.19	270.74 – 403.71	1.85 – 2.80	–	3.08 – 4.25	1.75 – 2.42	1.38 – 1.90	0.55 – 0.75
	QCTM	7.87 – 11.19	270.74 – 403.71	1.85 – 2.80	–	3.08 – 4.25	1.75 – 2.42	1.38 – 1.90	0.55 – 0.75
	TS2000	8.54	285.31	2.04	–	3.27	1.86	1.47	0.58
	ACCMIP	12.06	476.76	4.03	11.73	13.73	7.83	6.13	2.44
Anthropogenic non-traffic sources	EVAL2	32.88	364.66	88.03	–	3.15	5.43	1.33	8.40
	QCTM	32.88	364.66	88.03	–	3.15	5.43	1.33	8.40
	TS2000	32.88	364.66	88.03	–	3.15	5.43	1.33	8.40
	ACCMIP	32.88	364.66	88.03	36.27	3.15	5.43	1.33	8.40
Traffic sources	EVAL2	32.01 – 36.82	111.23 – 111.82	12.12 – 16.69	–	0.59 – 0.63	1.01 – 1.08	0.25 – 0.26	1.57 – 1.68
	QCTM	32.01 – 36.82	111.23 – 111.82	12.12 – 16.69	–	0.59 – 0.63	1.01 – 1.08	0.25 – 0.26	1.57 – 1.68
	TS2000	32.93	111.62	12.94	–	0.60	1.03	0.25	1.59
	ACCMIP	36.78	223.55	15.33	0.47	1.16	2.00	0.49	3.09
Natural sources (lightning)	EVAL2	23.66 (11.03)	112.80	30.69	–	11.38	0.54	3.42	0.35
	QCTM	16.52 (3.81)	112.80	30.69	–	11.38	0.54	3.42	0.35
	TS2000	23.50 (10.67)	112.80	30.69	–	11.38	0.54	3.42	0.35
	ACCMIP	25.31 (12.39)	112.80	30.69	–	11.38	0.54	3.42	0.35
Total	EVAL2	97.26 – 103.37	858.42 – 991.64	132.75 – 137.56	65.27	18.17 – 19.37	8.74 - 9.44	6.36 – 6.89	10.87 – 11.14
	QCTM	87.12 – 96.29	858.42 – 991.64	132.75 – 137.56	65.27	18.17 – 19.37	8.74 - 9.44	6.36 – 6.89	10.87 – 11.14
	TS2000	97.86	874.38	133.69	65.27	18.40	8.86	6.46	10.92
	ACCMIP	106.68	1177.77	138.08	48.46	29.43	15.80	11.36	14.28

Sector	**Experiment**	**C_4H_{10}**	**CH_3CHO**	**CH_3COCH_3**	**CH_3COOH**	**CH_3OH**	**HCHO**	**HCOOH**	**MEK**
Biomass and agric. waste burning	EVAL2	0.69 – 0.96	1.23 – 1.69	1.12 – 1.55	3.93 – 5.43	3.96 – 5.47	2.10 – 2.90	2.15 – 2.96	2.66 – 3.67
	QCTM	0.69 – 0.96	1.23 – 1.69	1.12 – 1.55	3.93 – 5.43	3.96 – 5.47	2.10 – 2.90	2.15 – 2.96	2.66 – 3.67
	TS2000	0.74	1.31	1.19	4.18	4.21	2.23	2.28	2.82
	ACCMIP	3.12	5.48	4.99	17.54	17.71	9.40	9.57	11.88
Anthropogenic non–traffic sources	EVAL2	62.82	–	2.78	–	2.78	0.87	–	3.75
	QCTM	62.82	–	2.78	–	2.78	0.87	–	3.75
	TS2000	62.82	–	2.78	–	2.78	0.87	–	3.75
	ACCMIP	62.82	–	2.78	–	2.78	0.87	–	3.75
Traffic sources	EVAL2	11.74 – 12.55	–	0.52 – 0.55	–	0.52 – 0.55	0.16 – 0.17	–	0.70 – 0.75
	QCTM	11.74 – 12.55	–	0.52 – 0.55	–	0.52 – 0.55	0.16 – 0.17	–	0.70 – 0.75
	TS2000	11.91	–	0.53	–	0.53	0.17	–	0.72
	ACCMIP	23.13	–	1.03	–	1.03	0.32	–	1.39
Natural sources	EVAL2	0.40	–	55.82	3.39	150.71	–	5.59	–
	QCTM	0.40	–	55.82	3.39	150.71	–	5.59	–
	TS2000	0.40	–	55.82	3.39	150.71	–	5.59	–
	ACCMIP	0.40	–	55.82	3.39	150.71	–	5.59	–
Total	EVAL2	75.65 – 76.54	1.23 – 1.69	60.12 – 60.58	7.32 – 8.82	157.63 – 159.16	3.13 – 3.94	7.72 – 8.54	7.11 – 8.15
	QCTM	75.65 – 76.54	1.23 – 1.69	60.12 – 60.58	7.32 – 8.82	157.63 – 159.16	3.13 – 3.94	7.72 – 8.54	7.11 – 8.15
	TS2000	75.87	1.31	60.32	7.57	158.22	3.27	7.87	7.29
	ACCMIP	89.48	5.48	64.61	20.93	172.22	10.59	15.16	17.02

S2 Additional figures

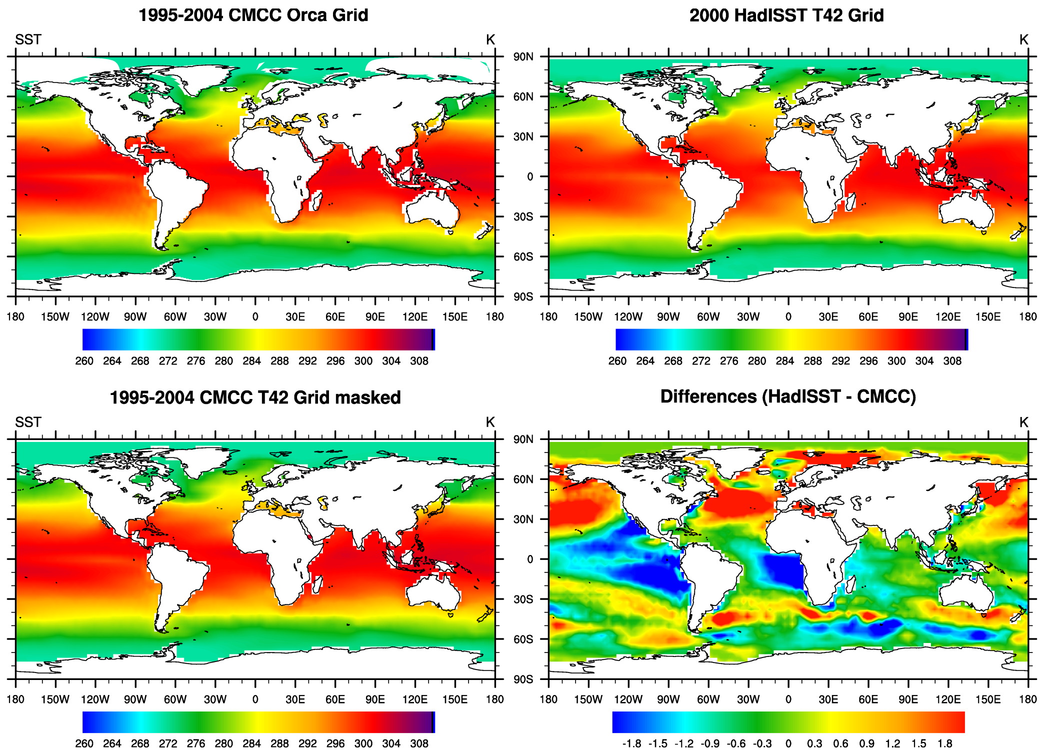

Figure S1: Annual mean sea surface temperature climatology in K (1995-2004) as simulated with the CMCC Climate Model (historical CMIP5 simulation) compared to HadISST used in the ACCMIP and TS2000 simulations, respectively. Top left: CMCC SICs on the ORCA coordinates interpolated to a T42 grid; Top right: HAdIIST data on a T42 grid; Bottom left: CMCC SICs in T42 masked with the ECHAM sea-land mask; Bottom right: differences between HAdIIST data on a T42 grid and CMCC SICs in T42 masked with the ECHAM sea-land mask.

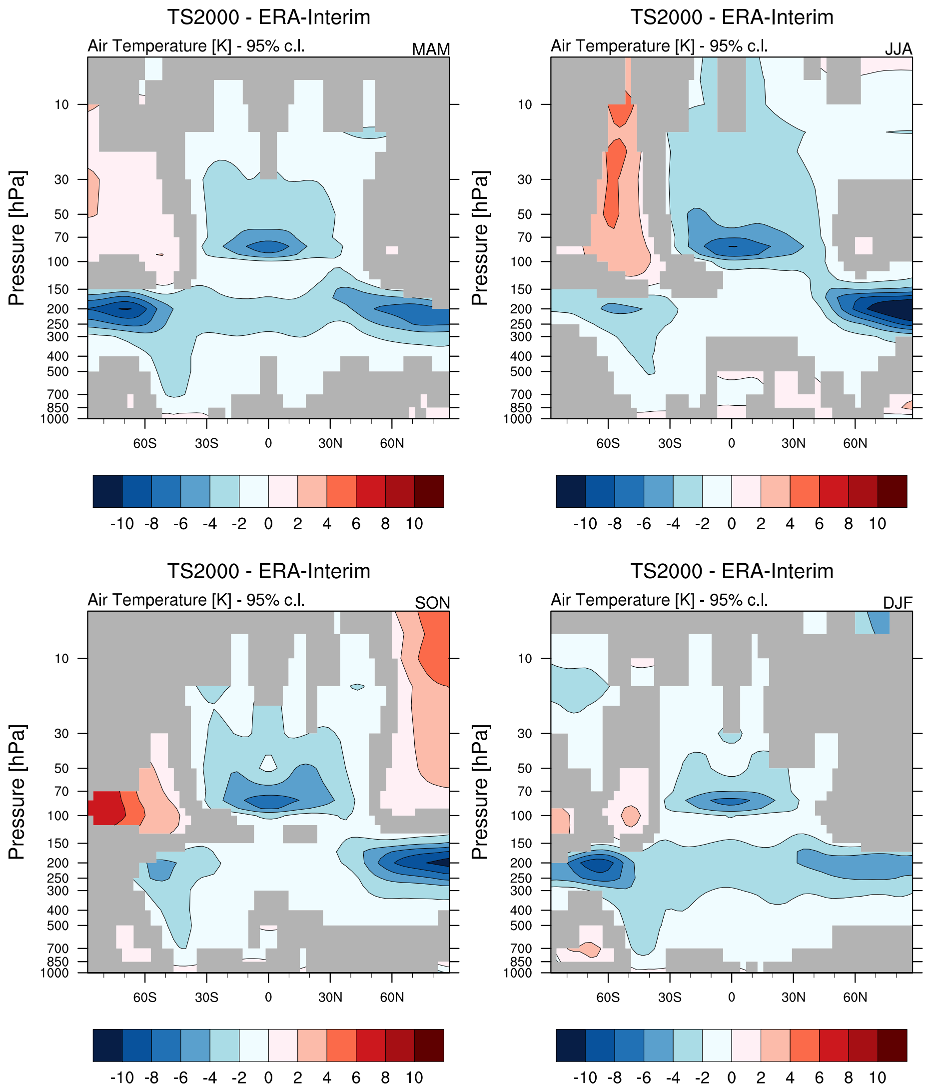

Figure S2: Seasonal mean of zonally averaged temperature profile for the TS2000 simulation in comparison to ERA-Interim. Clockwise from top-left: MAM, JJA, DJF, SON. Differences between the two fields that are not statistically significant according to the 95% confidence level are marked gray.

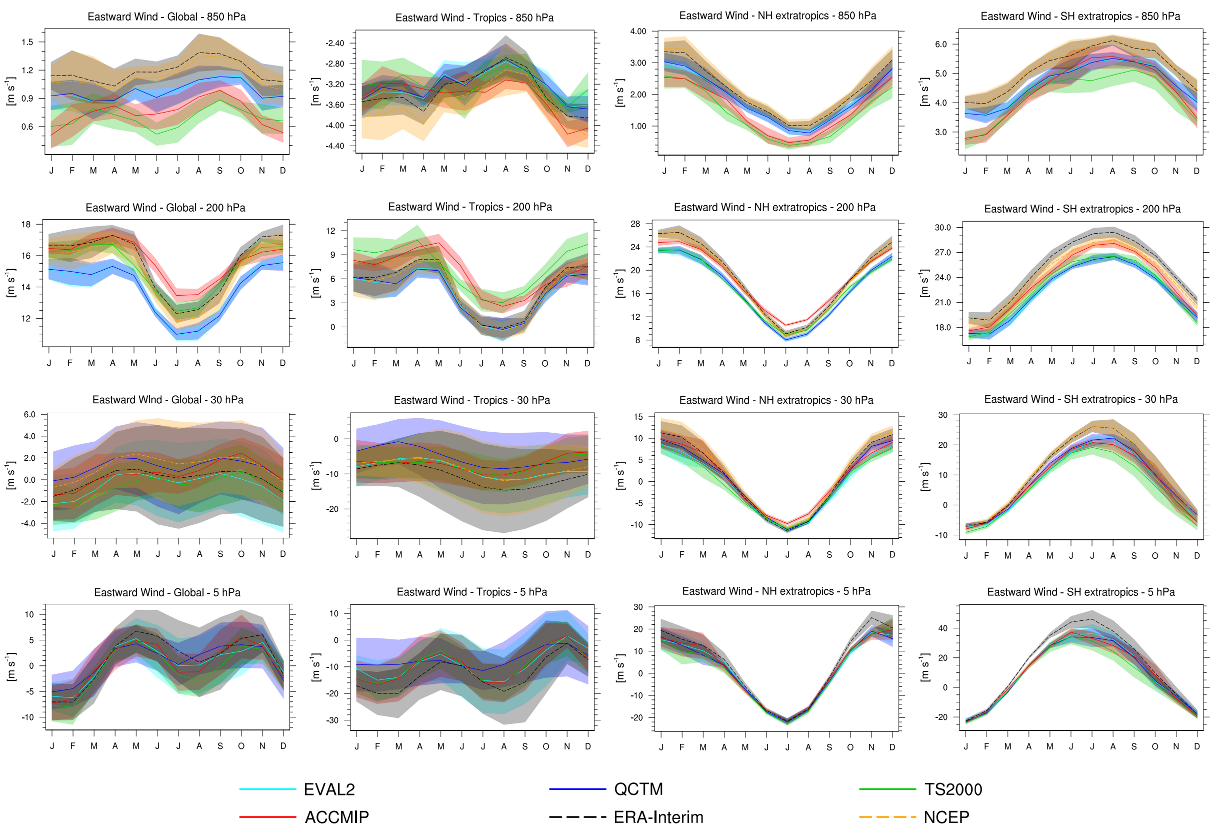

Figure S3: As in Fig. 1, for eastward wind.

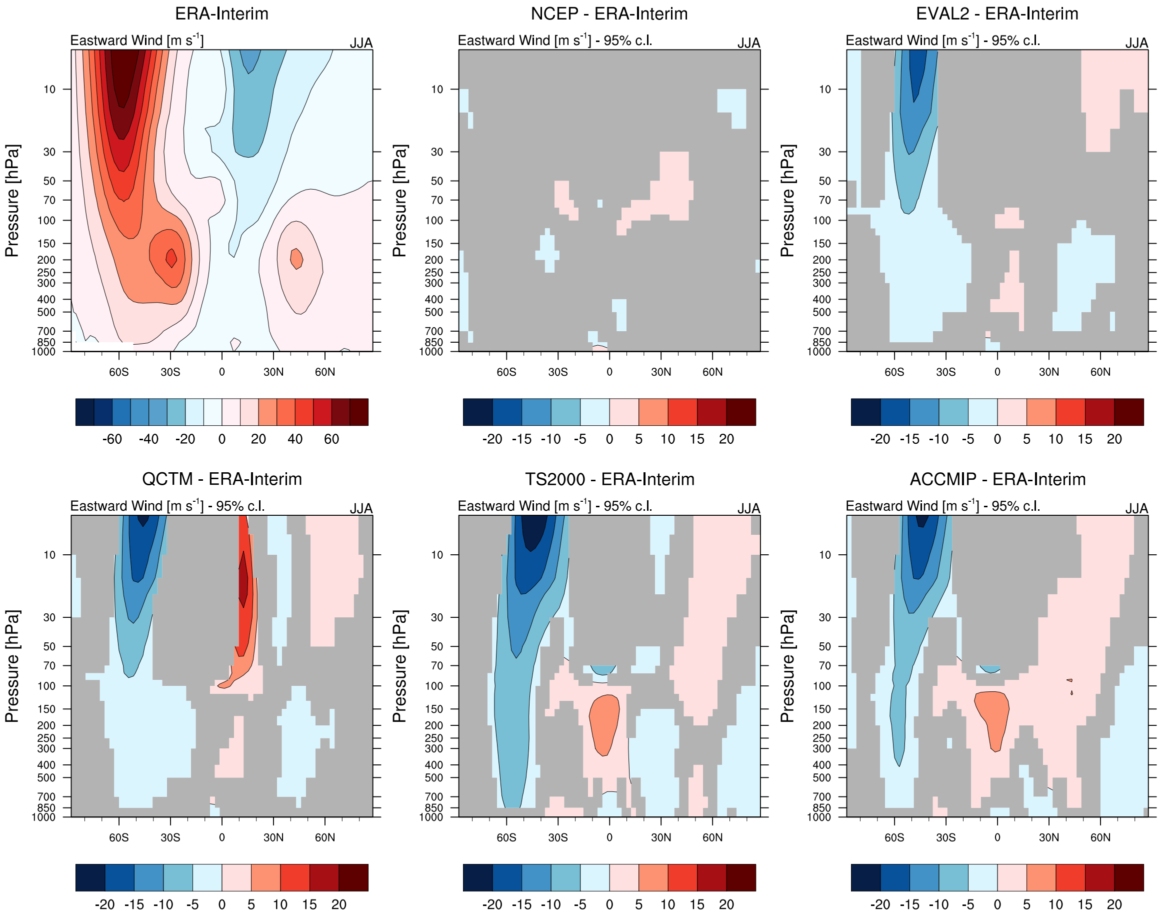

Figure S4: As in Fig. 8, for DJF mean.

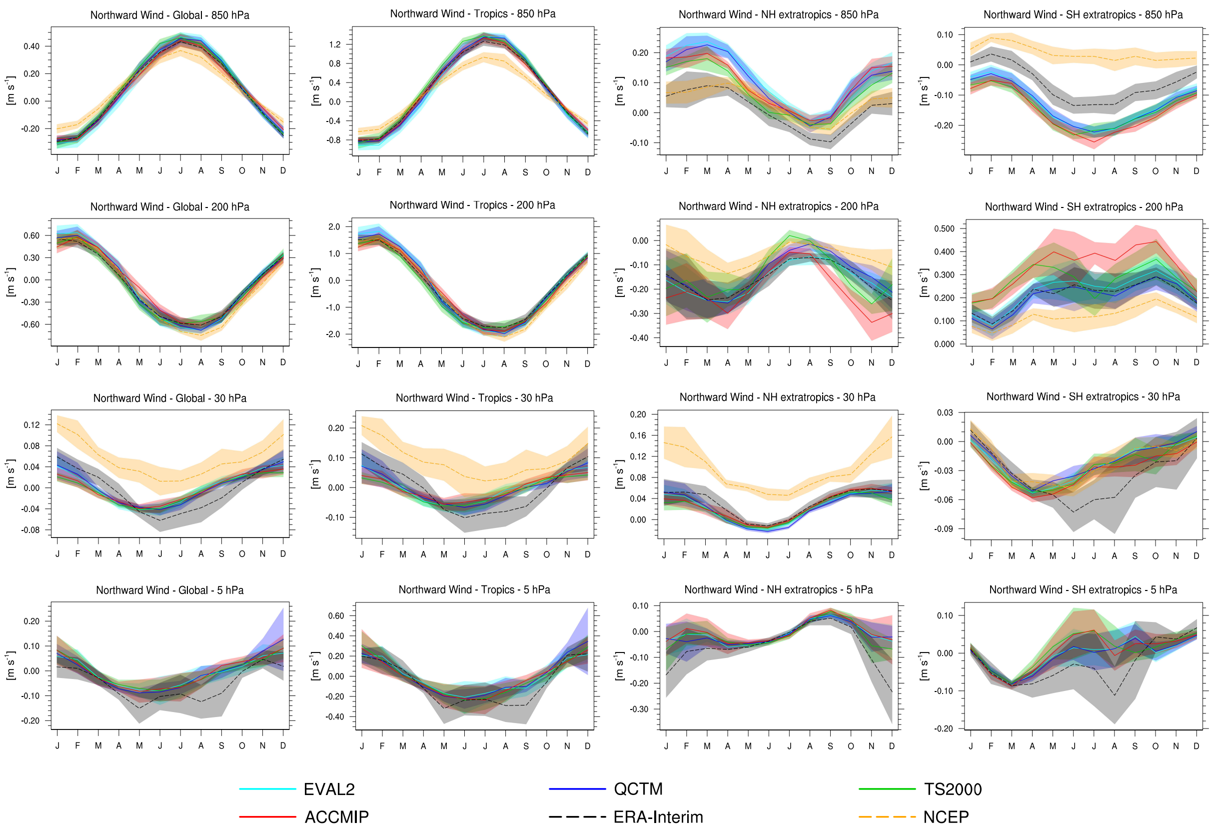

Figure S5: As in Fig. 1, for northward wind.

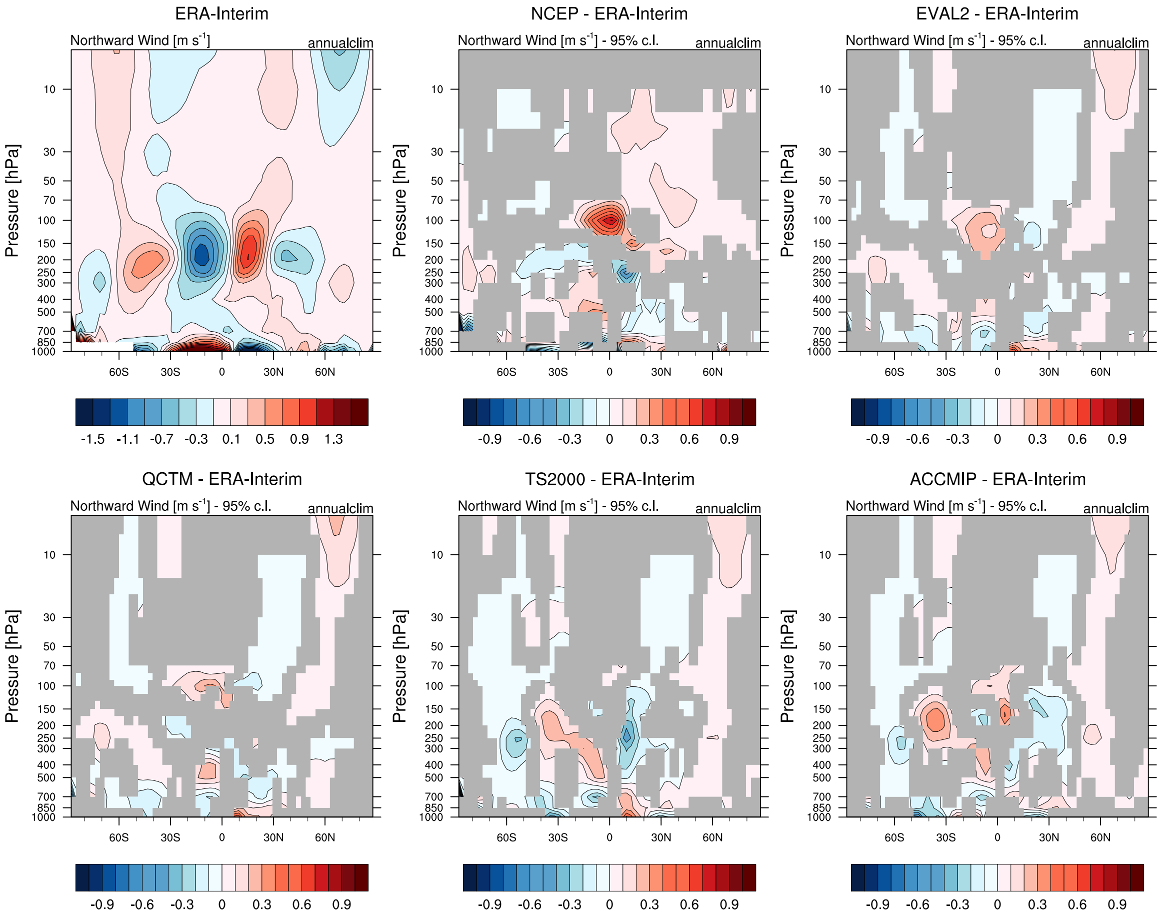

Figure S6: As in Fig. 2, for northward wind.

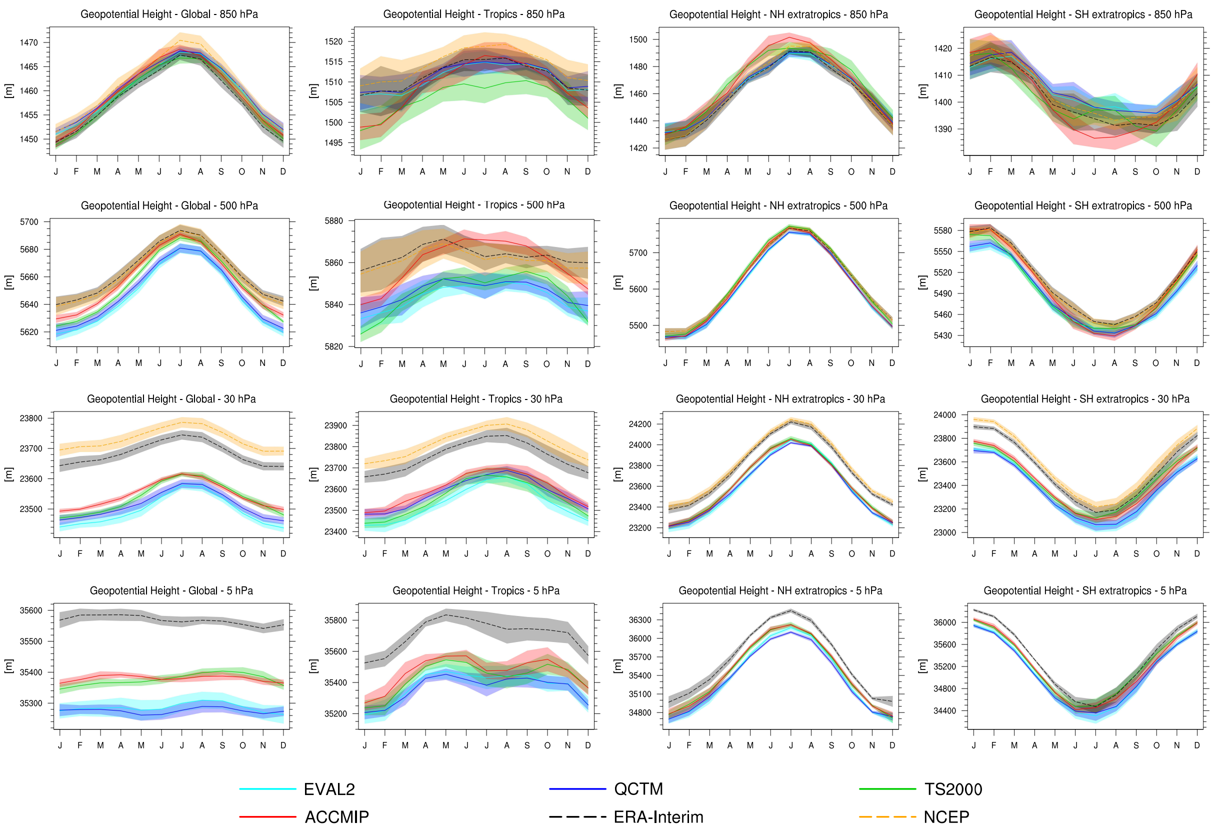

Figure S7: As in Fig. 1, for geopotential height. Note that the 500 hPa level in considered instead of 200.

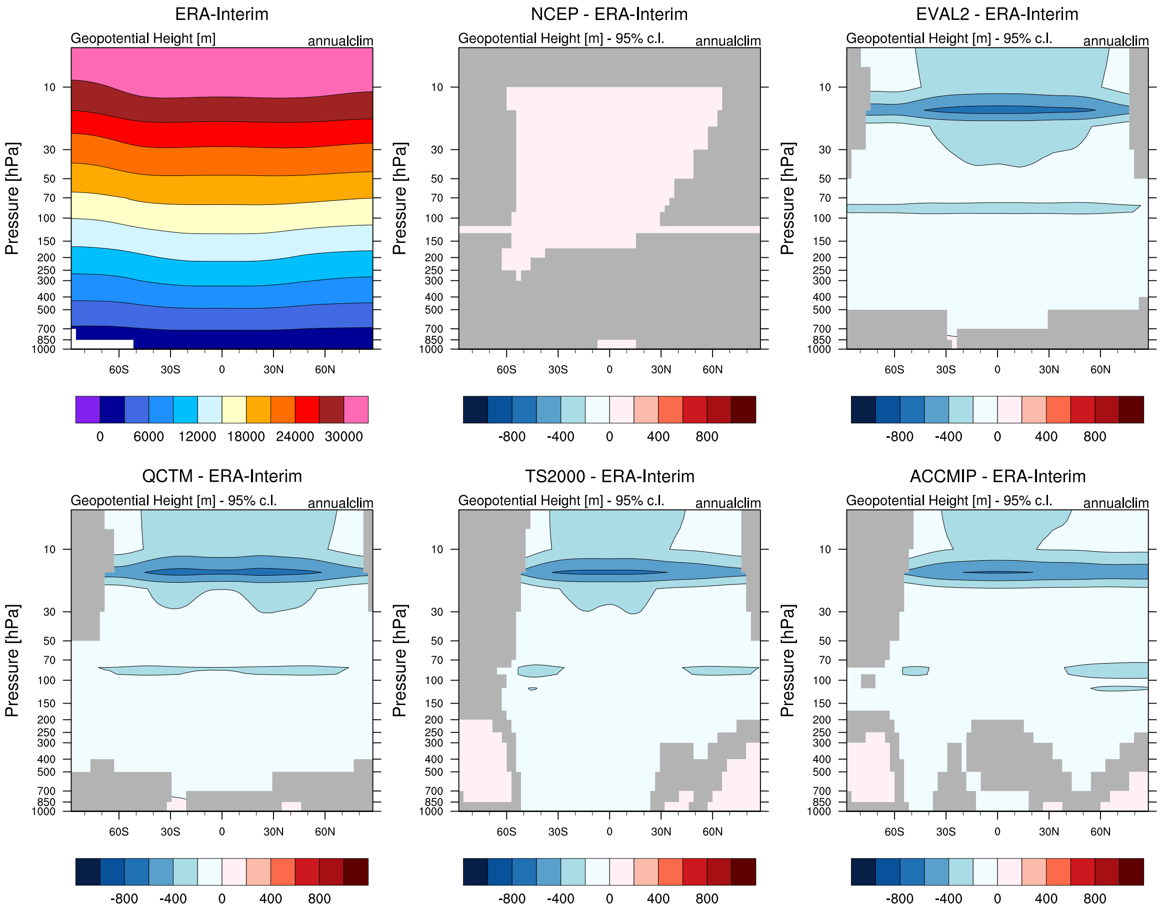

Figure S8: As in Fig. 2, for geopotential height.

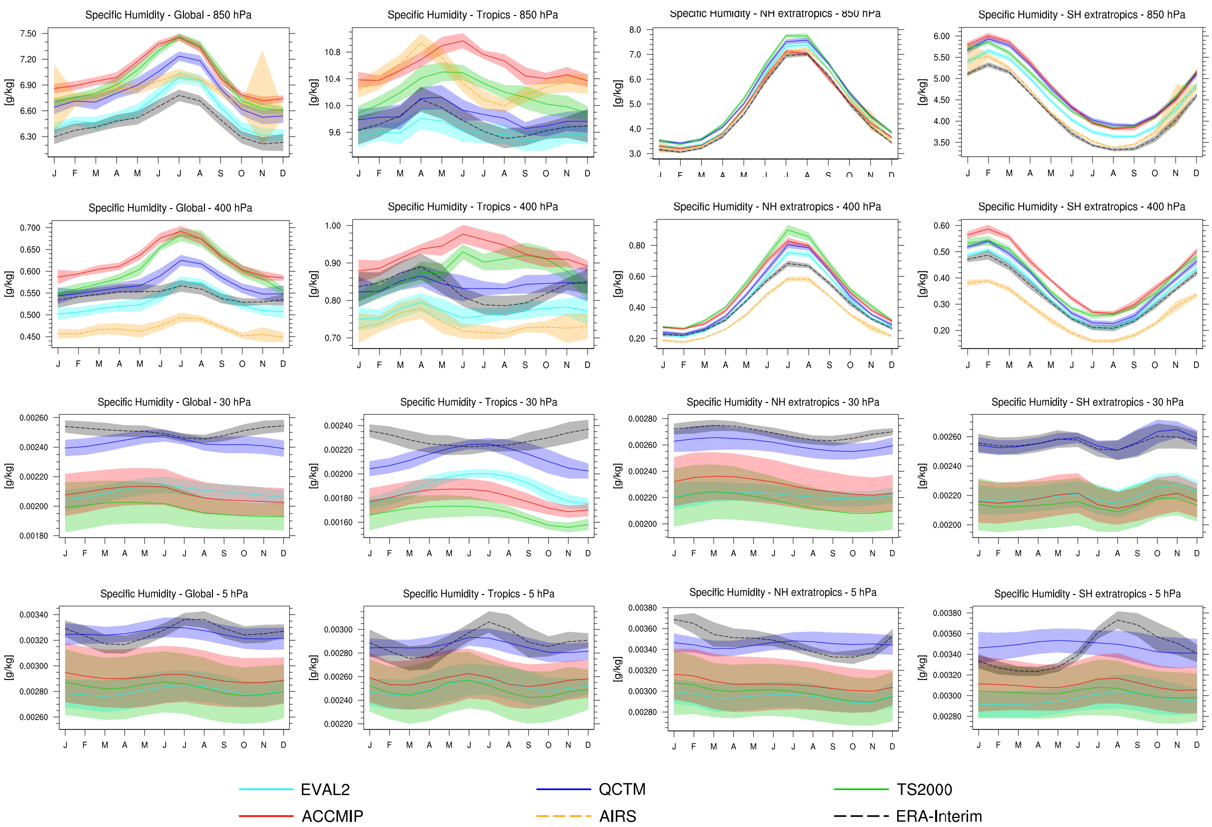

Figure S9: As in Fig. 1, for specific humidity. Note that the 400 hPa level in considered instead of 200.

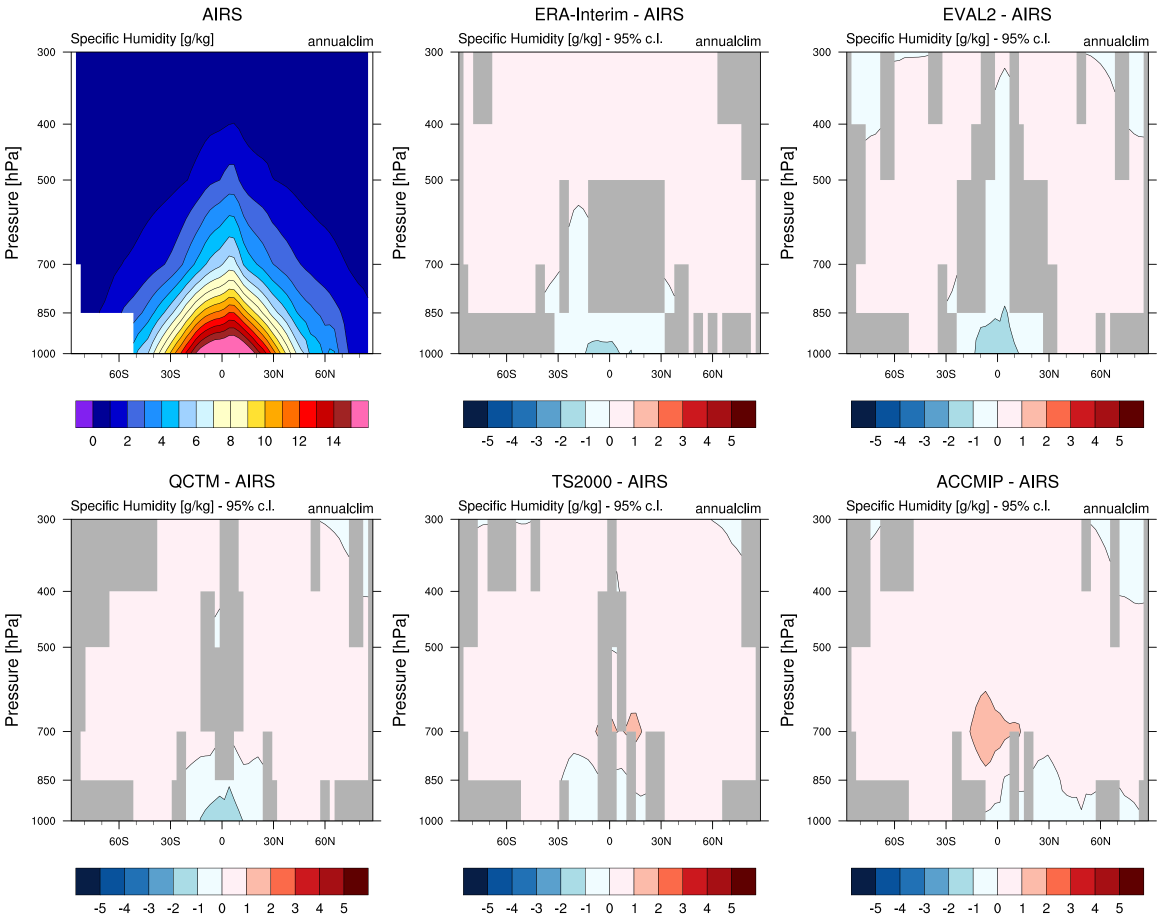

Figure S10: As in Fig. 2, for specific humidity.

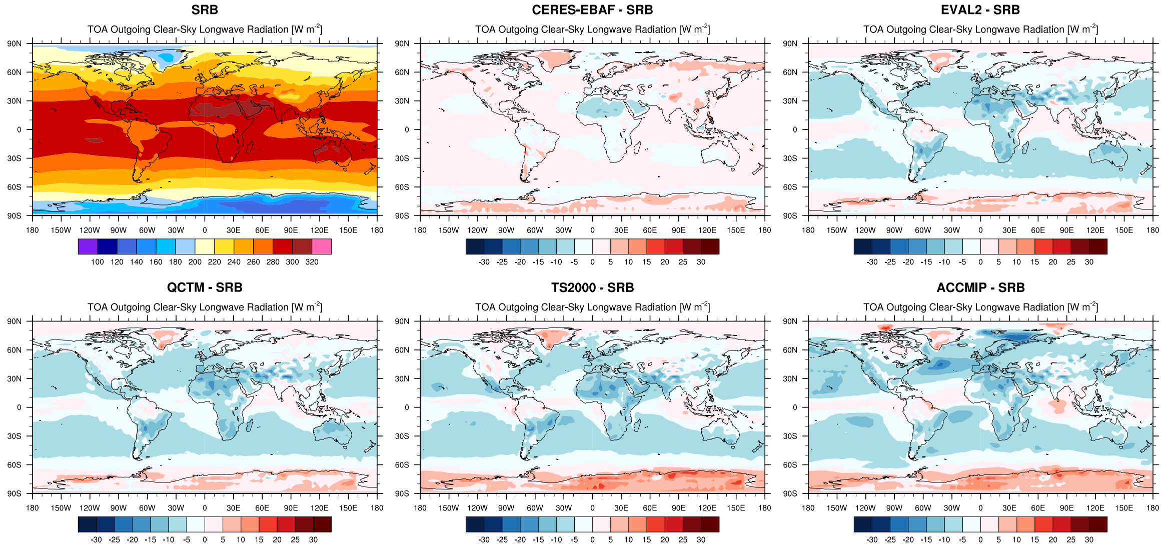

Figure S11: Annual mean clear-sky outgoing longwave radiation at TOA from SRB (upper left), differences from SRB data to CERES-EBAF data and to the EMAC simulations.

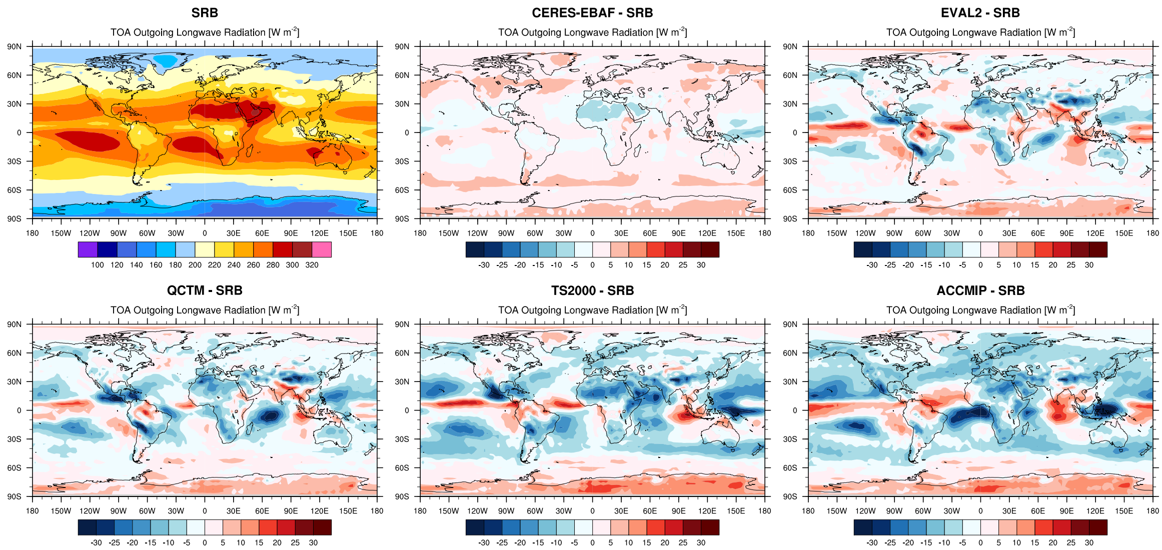

Figure S12: As in Fig. S11, for all-sky outgoing longwave radiation.

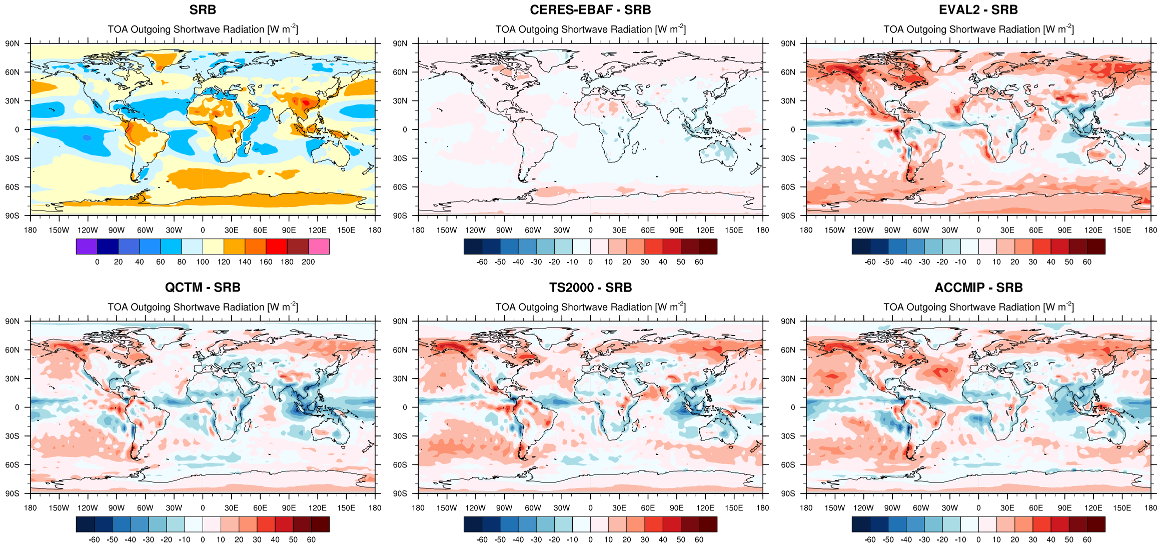

Figure S13: As in Fig. S11, for all-sky reflected shortwave radiation.

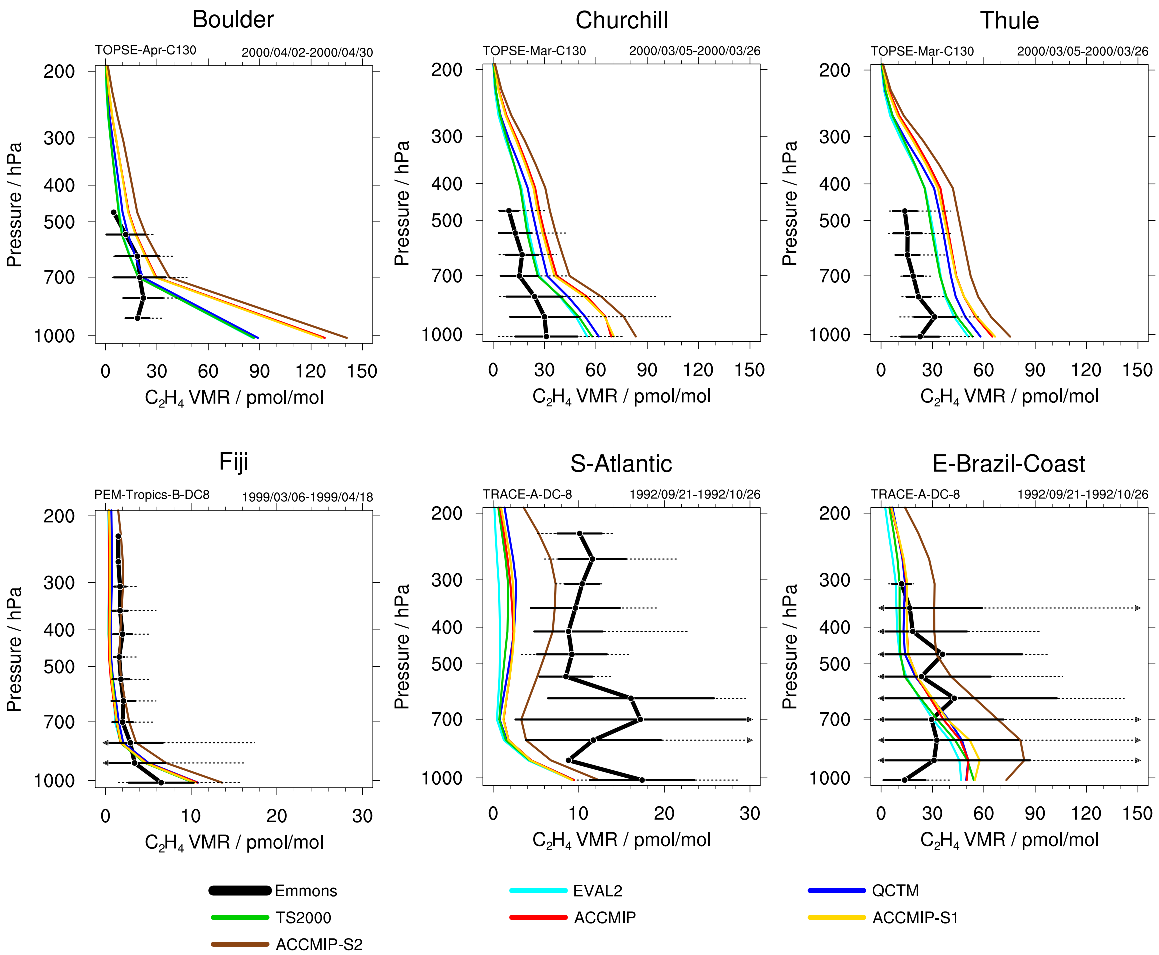

Figure S14: As in Fig. 16, for C_2H_4.

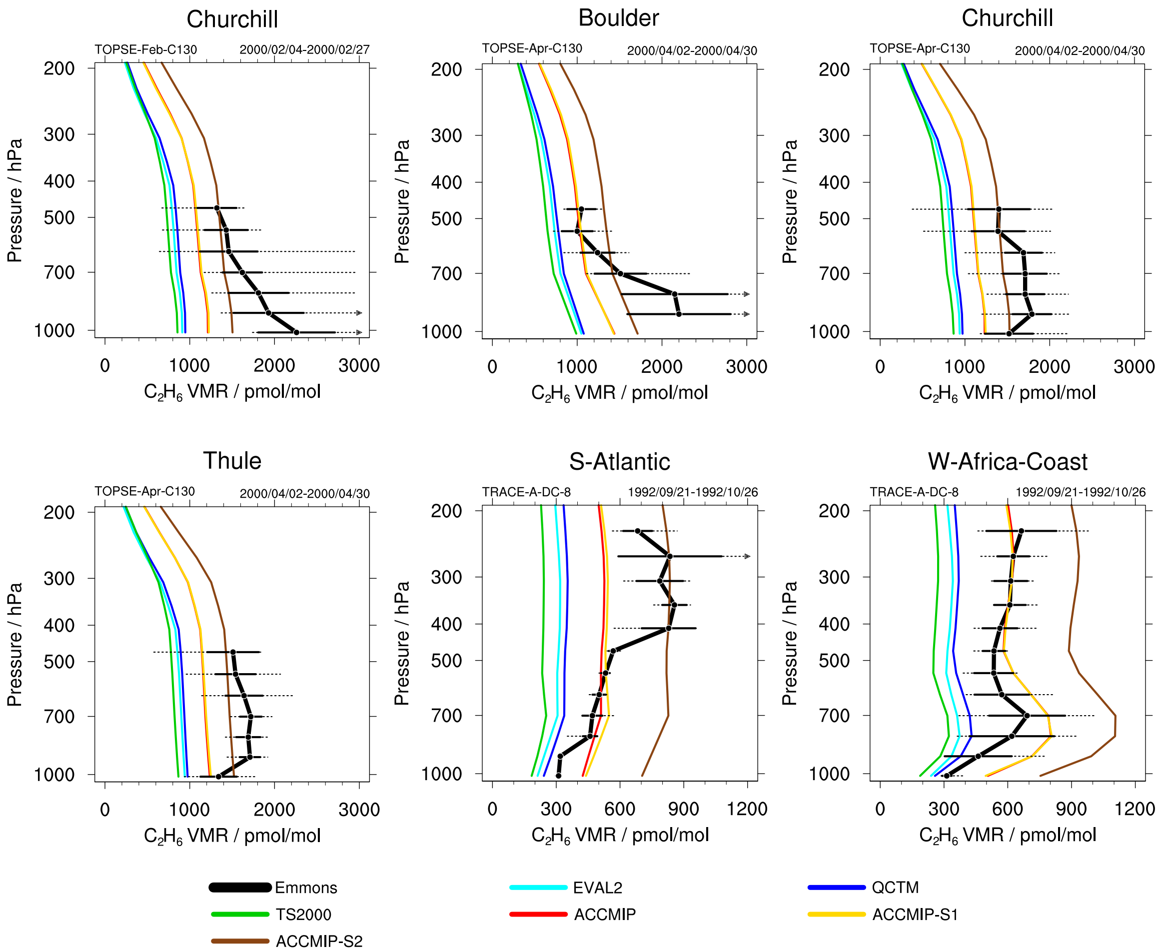

Figure S15: As in Fig. 16, for C_2H_6.

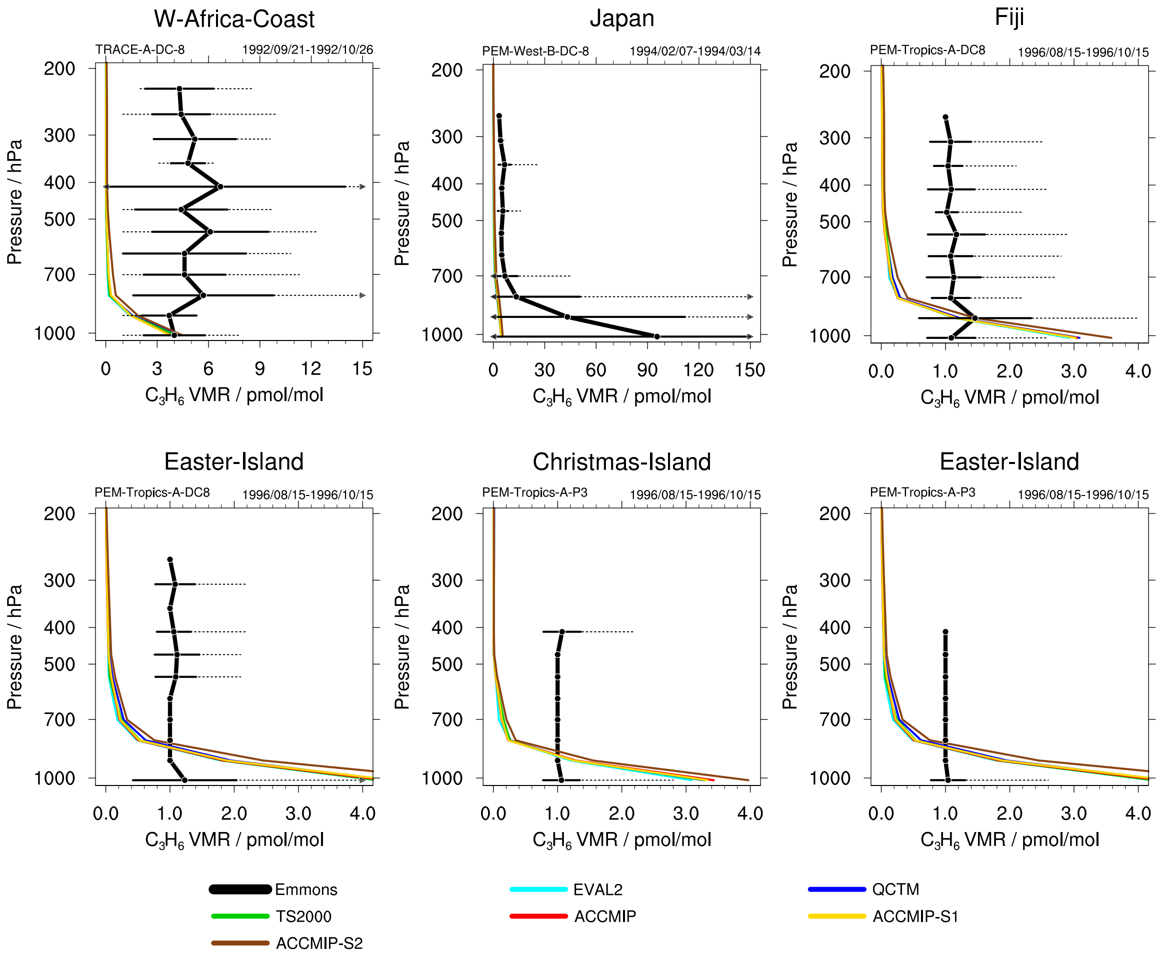

Figure S16: As in Fig. 16, for C_3H_6.

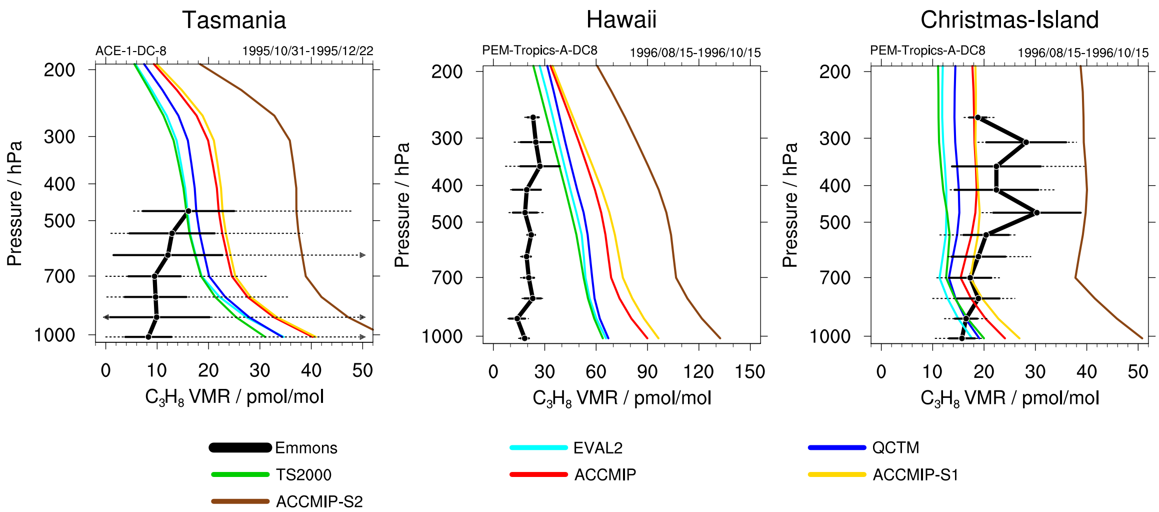

Figure S17: As in Fig. 16, for C_3H_8.

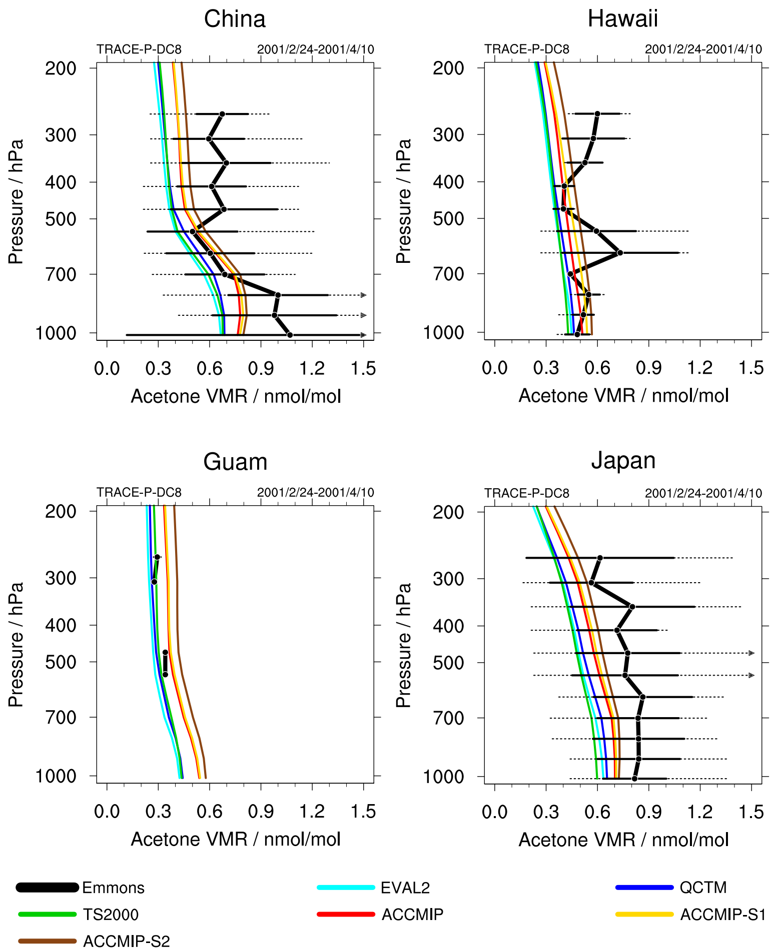

Figure S18: As in Fig. 17, for CH_3COCH_3 (acetone).

References

Boyer, T., Stephens, C., Antonov, J., Conkright, M., Locarnini, R., O'Brien, T., and Garcia, H.: World Ocean Atlas 2001, Volume 2 Salinity, NOOA Atlas NESDIS 50, U.S. Government Printing Office, 2002.

Broadgate, W. J., Liss, P. S., and Penkett, S. A.: Seasonal emissions of isoprene and other reactive hydrocarbon gases from the ocean, Geophys. Res. Lett., 24, 2675–2678, doi: 10.1029/97GL02736, 1997.

Dentener, F., Kinne, S., Bond, T. C., Boucher, O., Cofala, J., Generoso, S., Ginoux, P., Gong, S. L., Hoelzemann, J. J., Ito, A., Marelli, L., Penner, J. E., Putaud, J.-P., Textor, C., Schulz, M., van Der Werf, G. R., and Wilson, J.: Emissions of primary aerosol and precursor gases in the years 2000 and 1750 prescribed data-sets for AeroCom, Atmos. Chem. Phys., 6, 4321–4344, doi:10.5194/acp-6-4321-2006, 2006.

Emmons, L. K., Hauglustaine, D. A., Mller, J.-F., Carroll, M. A., Brasseur, G. P., Brunner, D., Staehelin, J., Thouret, V., and Marenco, A.: Data composites of airborne observations of tropospheric ozone and its precursors, J. Geophys. Res., 105, 20 497–20 538, doi: 10.1029/2000JD900232, 2000.

Giorgetta, M. A. and Bengtsson, L.: Potential role of the quasi-biennial oscillation in the stratosphere-troposphere exchange as found in water vapor in general circulation model experiments, J. Geophys. Res., 104, 6003–6019, doi:10.1029/1998JD200112, 1999.

Grewe, V., Brunner, D., Dameris, M., Grenfell, J., Hein, R., Shindell, D., and Staehelin, J.: Origin and variability of upper tropospheric nitrogen oxides and ozone at northern midlatitudes, Atmos. Environ., 35, 3421–3433, doi:10.1016/S1352-2310(01)00134-0, 2001.

Guenther, A., Hewitt, C. N., Erickson, D., Fall, R., Geron, C., Graedel, T., Harley, P., Klinger, L., Lerdau, M., Mckay, W. A., Pierce, T., B, S., Steinbrecher, R., Tallamraju, R., Taylor, J., and Zimmerman, P.: A global model of natural volatile organic compound emissions, J. Geophys. Res., 100, 8873–8892, doi:10.1029/94JD02950, 1995.

Hoor, P., Caro, D., Dessens, O., Endresen, O., Gauss, M., Grewe, V., Hauglustaine, D. A., Isaksen, I. S. A., Lelieveld, J., Myhre, G., Meijer, E., Olivie, D., Prather, M. J., Schnadt Poberaj, C., Shine, K. P., Staehelin, J., Tang, Q., van Aardenne, J. A., van Velthoven, P., and Sausen, R.: The impact of traffic emissions on atmospheric ozone and OH: results from QUANTIFY, Atmos. Chem. Phys., 9, 3113–3136, doi:10.5194/acp-9-3113-2009, 2009.

Kerkweg, A., Sander, R., Tost, H., and Jöckel, P.: Technical Note: Implementation of prescribed (OFFLEM), calculated (ONLEM), and pseudo-emissions (TNUDGE) of chemical species in the Modular Earth Submodel System (MESSy), Atmos. Chem. Phys., 6, 3603–3609, doi: 10.5194/acp-6-3603-2006, 2006.

Kettle, A. J. and Andreae, M. O.: Flux of dimethylsulfide from the oceans: A comparison of updated data sets and flux models, J. Geophys. Res., 105, 26 793–26 808, doi: 10.1029/2000JD900252, 2000.

Lamarque, J.-F., Bond, T. C., Eyring, V., Granier, C., Heil, A., Klimont, Z., Lee, D. S., Liousse, C., Mieville, A., Owen, B., Schultz, M. G., Shindell, D. T., Smith, S. J., Stehfest, E., van Aardenne, J. A., Cooper, O. R., Kainuma, M., Mahowald, N., McConnell, J. R., Naik, V., Riahi, K., and van Vuuren, D. P.: Historical (1850-2000) gridded anthropogenic and biomass burning emissions of reactive gases and aerosols: methodology and application, Atmos. Chem. Phys., 10, 7017–7039, doi:10.5194/acp-10-7017-2010, 2010.

Lean, J.: Evolution of the Sun's Spectral Irradiance Since the Maunder Minimum, Geophys. Res. Lett., 27, 2425–2428, doi:10.1029/2000GL000043, 2000.

Pozzer, A., Jöckel, P., Sander, R., Williams, J., Ganzeveld, L., and Lelieveld, J.: Technical Note: The MESSy-submodel AIRSEA calculating the air-sea exchange of chemical species, Atmos. Chem. Phys., 6, 5435–5444, doi:10.5194/acp-6-5435-2006, 2006.

Pozzer, A., Jöckel, P., and Van Aardenne, J.: The influence of the vertical distribution of emissions on tropospheric chemistry, Atmos. Chem. Phys., 2, 961–987, doi:10.5194/acp-12-961-2012, 2009.

Price, C. and Rind, D.: Modeling Global Lightning Distributions in a General Circulation Model, Mon. Wea. Rev., 122, 1930–1939, doi:0.1175/1520-0493(1994)122¡1930:MGLDIA¿2.0.CO;2, 1994.

Prinn, R. G., Weiss, R. F., Fraser, P. J., Simmonds, P. G., Cunnold, D. M., Alyea, F. N., Doherty, S. O., Salameh, P., Miller, B. R., Huang, J., Wang, R. H. J., Hartley, D. E., Harth, C., Steele, L. P., Sturrock, G., Midgley, P. M., and McCulloch, A.: A history of chemically and radiatively important gases in air deduced from ALE/GAGE/AGAGE, J. Geophys. Res., 105, 17 751–17 792, doi:10.1029/2000JD900141, 2000.

Schmitt, A. and Brunner, B.: Emissions from aviation and their development over time, in: Pollutants from Air Traffic - Results of Atmospheric Research 19921997, edited by Schumann, U., Chlond, A., Ebel, A., Krcher, B., Pak, H., Schlager, H., Schmitt, A., and Wendling, P., pp. 37–52, DLR-Mitteilung 97-04, Deutsches Zentrum fr Luft- und Raumfahrt, Cologne, Germany, 1997.

Spiro, P. A., Jacob, D. J., and Logan, J. A.: Global inventory of sulfur emissions with $1^\circ \times 1^\circ$ resolution, J. Geophys. Res., 97, 6023–6036, doi:10.1029/91JD03139, 1992.

Tanre, D., Geleyn, J.-F., and Slingo, J.: First results of the introduction of an advanced aerosol-radiation interaction in the ECMWF low resolution global model, in: Aerosols and their climatic effects, edited by Gerber, H. and Deepak, A., pp. 133–177, A. Deepak Publ., 1994.

Vignati, E., Wilson, J., and Stier, P.: M7: An efficient size-resolved aerosol microphysics module for large-scale aerosol transport models, J. Geophys. Res., 109, doi:10.1029/2003JD004485, 2004.

von Kuhlmann, R., Lawrence, M. G., Crutzen, P. J., and Rasch, P. J.: A model for studies of tropospheric ozone and nonmethane hydrocarbons: Model description and ozone results, J. Geophys. Res., 108, 4294, doi:10.1029/2002JD002893, 2003.